Carbon Dioxide Coordination and Activation by Niobium Oxide Molecules

ARTICLE *in* THE JOURNAL OF PHYSICAL CHEMISTRY A · NOVEMBER 2011

Impact Factor: 2.69 · DOI: 10.1021/jp208291g · Source: PubMed

THE JOURNAL OF PHYSICAL CHEMISTRY A

ARTICLE

pubs.acs.org/JPCA

Carbon Dioxide Coordination and Activation by Niobium Oxide Molecules

Mingfei Zhou,*[,†] Zijian Zhou,[‡] Jia Zhuang,[†] Zhen Hua Li,*[,†] Kangnian Fan,[†] Yanying Zhao,[‡] and Xuming Zheng[‡]

[†]Department of Chemistry, Shanghai Key Laboratory of Molecular Catalysts and Innovative Materials, Fudan University, Shanghai 200433, China

[‡]Department of Chemistry, Zhejiang Sci-Tech University, Hangzhou, China

ABSTRACT: Carbon dioxide coordination and activation by niobium oxide molecules were studied by matrix isolation infrared spectroscopy. It was found that the niobium monoxide molecule reacted with carbon dioxide to form the niobium dioxide carbonyl complex $NbO_2(\eta^1\text{-}CO)$ spontaneously on annealing in solid neon. The observation of the spontaneous reaction is consistent with theoretical predictions that this carbon dioxide activation process is both thermodynamically exothermic and kinetically facile. In contrast, four niobium dioxide−carbon dioxide complexes exhibiting three different coordination modes of CO_2 were formed from the reactions between niobium dioxide and carbon dioxide, which proceeded with the initial formation of the η^1-O bound $NbO_2(\eta^1\text{-}OCO)$ and $NbO_2(\eta^1\text{-}OCO)_2$ complexes on annealing. The $NbO_2(\eta^1\text{-}OCO)$ complex rearranged to the η^2-O,O bound $NbO_2(\eta^2\text{-}O_2C)$ isomer under visible light irradiation, while the $NbO_2(\eta^1\text{-}OCO)_2$ complex isomerized to the $NbO_2(\eta^1\text{-}OCO)(\eta^2\text{-}OC)O$ structure involving an η^2-C,O ligand under IR excitation. In these niobium dioxide carbon dioxide complexes, the η^1-O coordinated CO_2 ligand serves as an electron donor, whereas both the η^2-C,O and η^2-O,O coordinated CO_2 ligands act as electron acceptors.

INTRODUCTION

The chemical transformation of the greenhouse gas CO_2 into useful compounds is receiving increased attention.[1] Due to its kinetic and thermodynamic stability, efforts to convert CO_2 to useful chemicals will rely on its activation through catalysts, particularly transition metal catalysts.[2,3] The interactions of transition metal atoms, cations, and anions, as well as simple metal oxide molecules, with CO_2 serve as the simplest model in understanding the intrinsic mechanism of catalytic CO_2 activation processes.

Previous gas phase kinetic studies on the reactions between atomic transition metal cations and CO_2 have shown that early transition metal cations are able to activate CO_2 in forming metal monoxide cation and CO, whereas the other transition metal cations form adducts with CO_2.[4−9] Matrix isolation spectroscopic as well as gas phase kinetic investigations have been performed on the reactions of neutral transition metal atoms with CO_2, which indicated that the ground state early transition metal atoms were able to activate the C═O bond of CO_2 in forming the inserted OMCO molecules, while the late transition metal atoms interacted with CO_2 to give either the η^1-C or η^1-O coordination complexes.[10−18] Besides the experimental studies, quantum chemical calculations have also been performed to understand the reaction mechanisms as well as the structural and bonding properties of the resulting complexes.[19−23] By contrast, the reactions between transition metal oxides and carbon dioxide have received much less attention. The reactivity of simple transition metal oxide cations such as monoxide cations with CO_2 has been studied in the gas phase. The MO_2^+ dioxide formation by O atom transfer occurred only with NbO^+, HfO^+, TaO^+, and WO^+.[8,9] CO_2 reduction by group 6 transition metal suboxide cluster anions was reported.[24] In this paper, CO_2 coordination and activation by niobium oxide molecules were studied. The results showed that the niobium monoxide molecule is able to activate carbon dioxide to form $NbO_2(\eta^1\text{-}CO)$ in solid neon; in contrast, the niobium dioxide molecule reacted with carbon dioxide to form four niobium dioxide−carbon dioxide complexes exhibiting three different coordination modes of CO_2, which provide as an ideal prototype system in understanding the metal−carbon dioxide interactions.

EXPERIMENTAL AND COMPUTATIONAL METHODS

The reactions were studied by matrix isolation infrared spectroscopy. The niobium monoxide and dioxide molecules were prepared by pulsed laser evaporation of bulk niobium oxide target. Recent investigations in our laboratory have shown that pulsed laser evaporation is an effective method in preparing transition metal monoxide or dioxide molecules for matrix isolation spectroscopic studies.[25−27] The experimental setup for pulsed laser-evaporation and matrix isolation infrared spectroscopic investigation has been described in detail

Received: August 27, 2011
Revised: November 7, 2011
Published: November 07, 2011

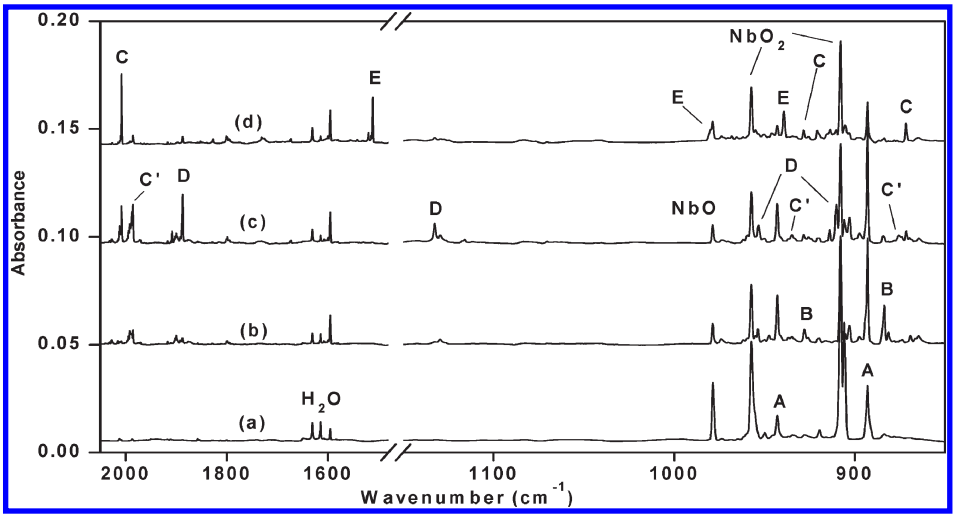

Figure 1. Infrared spectra in the 2050−1480 and 1150−850 cm^{-1} regions from codeposition of laser-evaporated niobium oxides with 0.2% CO_2 in neon: (a) after 30 min of sample deposition at 4 K, (b) after 12 K annealing, (c) after 20 min of near IR ($\lambda > 800$ nm) irradiation, and (d) after 20 min of visible ($400 < \lambda < 580$ nm) irradiation.

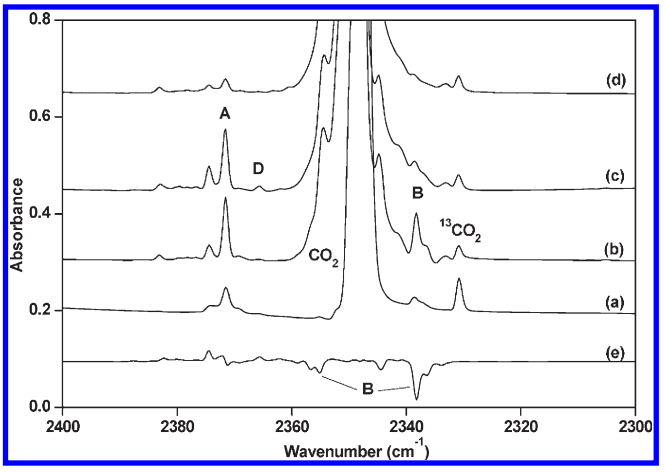

Figure 2. Infrared spectra in the 2400−2300 cm^{-1} region from codeposition of laser-evaporated niobium oxides with 0.2% CO_2 in neon: (a) after 30 min of sample deposition at 4 K, (b) after 12 K annealing, (c) after 20 min of near IR irradiation ($\lambda > 800$ nm), (d) after 20 min of visible light irradiation ($400 < \lambda < 580$ nm), and (e) difference spectrum of (c − b).

previously.[28] Briefly, the 1064 nm fundamental of a Nd:YAG laser (Continuum, Minilite II, 10 Hz repetition rate and 6 ns pulse width) was focused onto a rotating niobium oxide target through a hole in a CsI window cooled normally to 4 K - by means of a closed-cycle helium refrigerator. The laser-evaporated metal oxide species were codeposited with CO_2/Ne mixtures onto the CsI window. In general, matrix samples were deposited for 30 min at a rate of approximately 4 mmol/h. The bulk Nb_2O_5 target was prepared from sintered metal oxide powder. The CO_2/Ne mixtures were prepared in a stainless steel vacuum line using standard manometric technique. Isotopically labeled $^{13}CO_2$ (Spectra Gases Inc., 99%), $C^{18}O_2$ (Cambridge Isotopic Laboratories, 95%) and $C^{16}O_2 + C^{16}O^{18}O + C^{18}O_2$ (Cambridge Isotopic Laboratories, 61% ^{18}O) were used without further purification. The infrared absorption spectra of the resulting samples were recorded on a Bruker IFS 80 V spectrometer at 0.5 cm^{-1} resolution between 4000 and 450 cm^{-1} using a liquid nitrogen cooled HgCdTe (MCT) detector. Samples were annealed to different temperatures and cooled back to 4 K for spectral acquisition, and selected samples were subjected to broad band irradiation using a tungsten lamp or a high-pressure mercury arc lamp with glass filters.

Quantum chemical calculations were performed to determine the molecular structures and to support the assignment of vibrational frequencies of the observed reaction products. Calculations were performed using the hybrid B3LYP functional with the 6-311+G(d) basis set for the C and O atoms and the SDD pseudo potential and basis set for Nb.[29,30] The geometries were fully optimized, and the harmonic vibrational frequencies were calculated with analytic second derivatives. The zero-point energies (ZPE) were derived. Transition state optimizations were done with the synchronous transit-guided quasi-Newton (STQN) method and were verified through intrinsic reaction coordinate (IRC) calculations. All these calculations were performed by using the Gaussian 09 program.[31]

RESULTS AND DISCUSSION

Pulsed laser evaporation of bulk Nb_2O_5 target under controlled laser energy (2−5 mJ/pulse) followed by condensation with pure neon formed only the NbO (978.5 cm^{-1}) and NbO_2 (ν_3, 907.8 cm^{-1}; ν_1, 957.2 cm^{-1}) molecules.[32] The spectra in selected regions from codeposition of laser-evaporated niobium monoxide and dioxide molecules with 0.2% CO_2 in neon are shown in Figures 1−3, respectively. Besides the CO_2 absorptions, the NbO and NbO_2 absorptions dominated the spectrum after sample deposition at 4 K. Three groups of product absorptions were increased (labeled as **A**, **B**, and **C** in Figures 1−3) upon sample annealing at the expense of the niobium oxide absorptions. When the sample was subjected to broad-band near IR irradiation ($\lambda > 800$ nm), the group **B** absorptions were almost destroyed with the production of a new group of absorptions (labeled as **D** in Figures 1 and 2). When the sample was subjected to additional visible light irradiation ($400 < \lambda < 580$ nm), both the

dx.doi.org/10.1021/jp208291g |J. Phys. Chem. A 2011, 115, 14361–14369

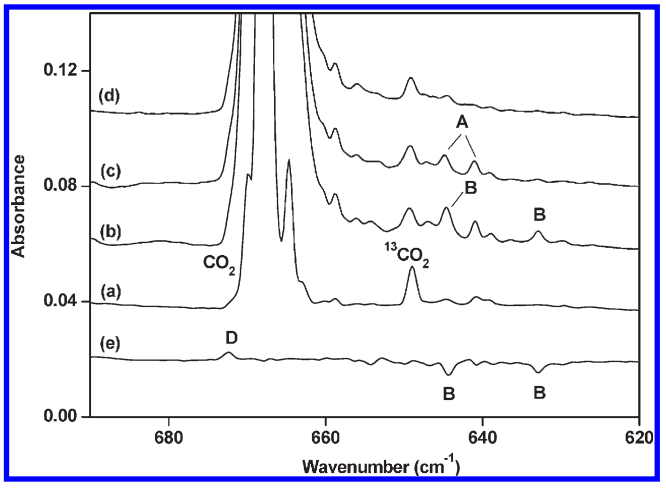

Figure 3. Infrared spectra in the 690−620 cm^{-1} region from codeposition of laser-evaporated niobium oxides with 0.2% CO_2 in neon: (a) after 30 min of sample deposition at 4 K, (b) after 12 K annealing, (c) after 20 min of near IR irradiation ($\lambda > 800$ nm), (d) after 20 min of visible light irradiation ($400 < \lambda < 580$ nm), and (e) difference spectrum of (c − b).

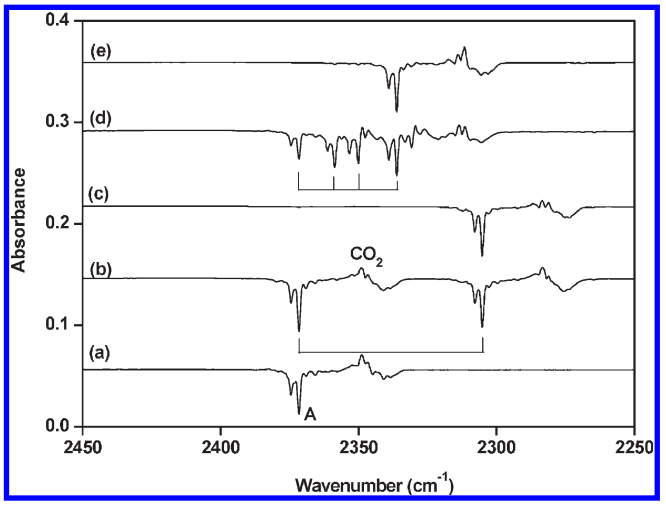

Figure 4. Difference infrared spectra in the 2450−2250 cm^{-1} region from codeposition of laser-evaporated niobium oxides with isotopic-labeled CO_2 in excess neon (spectrum taken after 20 min of $300 < \lambda < 580$ nm irradiation minus spectrum after 20 min of $\lambda > 500$ nm irradiation): (a) 0.1% CO_2, (b) 0.05% $^{12}CO_2$ + 0.05% $^{13}CO_2$, (c) 0.1% $^{13}CO_2$, (d) 0.1% ($C^{16}O_2$ + $C^{16}O^{18}O$ + $C^{18}O_2$), 61% ^{18}O, and (e) 0.1% $C^{18}O_2$.

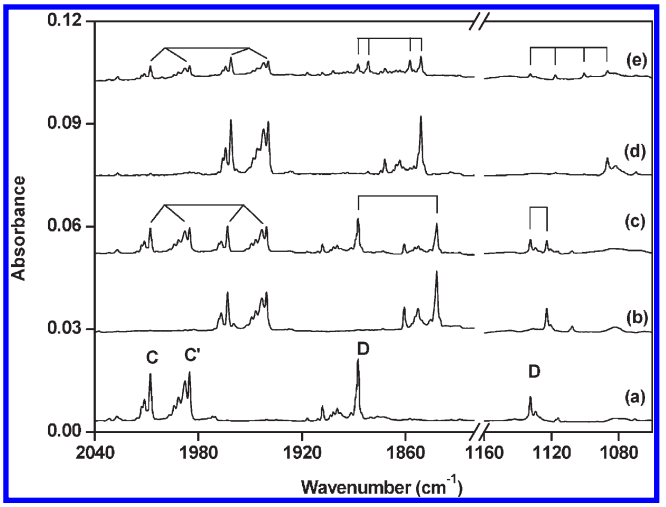

Figure 5. Infrared spectra in the 2040−1820 and 1160−1060 cm^{-1} regions from codeposition of laser-evaporated niobium oxides with isotopic-labeled CO_2 in excess neon. Spectra were taken after 30 min of sample deposition, followed by 12 K annealing and near IR irradiation: (a) 0.2% CO_2, (b) 0.2% $^{13}CO_2$, (c) 0.1% $^{12}CO_2$ + 0.1% $^{13}CO_2$, (d) 0.2% $C^{18}O_2$, and (e) 0.2% ($C^{16}O_2$ + $C^{16}O^{18}O$ + $C^{18}O_2$), 61% ^{18}O.

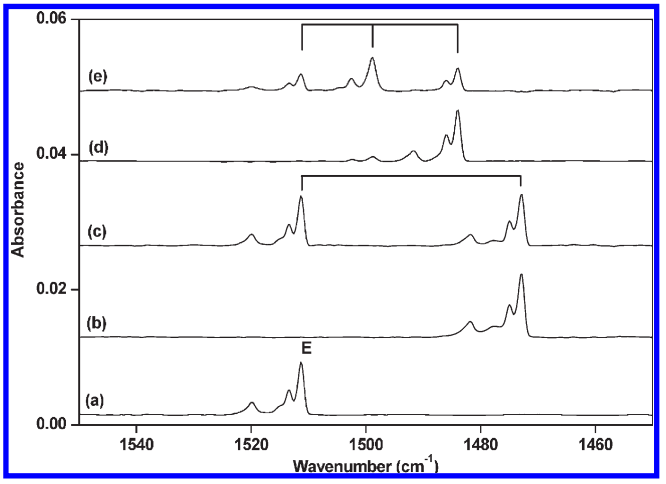

Figure 6. Infrared spectra in the 1550−1450 cm^{-1} region from codeposition of laser-evaporated niobium oxides with isotopic-labeled CO_2 in excess neon (spectra were taken after 30 min of sample deposition, followed by 12 K annealing and visible light irradiation): (a) 0.2% CO_2, (b) 0.2% $^{13}CO_2$, (c) 0.1% $^{12}CO_2$ + 0.1% $^{13}CO_2$, (d) 0.2% $C^{18}O_2$, and (e) 0.2% ($C^{16}O_2$ + $C^{16}O^{18}O$ + $C^{18}O_2$), 61% ^{18}O.

group **A** and **D** absorptions were destroyed, while a group of new absorptions (labeled as **E**) were produced. The same product absorptions were observed but with different relative intensities in similar experiments with different CO_2 concentrations (ranging from 0.02 to 0.2%). The **B** and **D** absorptions are favored with relatively high CO_2 concentrations with respect to the **A**, **C**, and **E** absorptions. The spectra from the experiments with isotopic-labeled samples ($^{13}CO_2$, $^{12}CO_2$ + $^{13}CO_2$, $C^{18}O_2$ and $C^{16}O_2$ + $C^{16}O^{18}O$ + $C^{18}O_2$) are shown in Figures 4−6. The vibrational frequencies and assignments are listed in Table 1.

All of the above-mentioned product absorptions should be assigned to niobium dioxide complexes (Table 1). Each product exhibits two absorptions in the NbO stretching frequency region, which are due to symmetric and antisymmetric NbO_2 stretching modes. The group **A** absorptions are assigned to the 1:1 $NbO_2(\eta^1\text{-OCO})$ complex with CO_2 coordinated to the Nb center in an η^1-O end-on fashion (Table 1). The 2371.5, 1376.1, and 641.0 cm^{-1} absorptions are attributed to the antisymmetric stretching, symmetric stretching and bending vibrations of the CO_2 subunit. The spectral feature observed in the experiment with the $^{12}CO_2$ + $^{13}CO_2$ mixture (Figure 4, trace b) clearly indicates that only one CO_2 subunit is involved in species **A**. The antisymmetric CO_2 stretching mode split into four absorptions at 2371.5, 2358.6, 2350.1, and 2336.1 cm^{-1} using the $C^{16}O_2$ + $C^{16}O^{18}O$ + $C^{18}O_2$ sample (Figure 4, trace d), indicating that the two O atoms in the CO_2 subunit are

dx.doi.org/10.1021/jp208291g |J. Phys. Chem. A 2011, 115, 14361–14369

Table 1. Observed Vibrational Frequencies (cm^{-1}) for the Niobium Dioxide Complexes in Solid Neon

$^{12}C^{16}O_2$	$^{13}C^{16}O_2$	$^{12}C^{18}O_2$	assignment
2371.5	2305.0	2336.1	**A** antisym. CO_2 str.
1376.1	1366.8	1318.9	**A** sym. CO_2 str.
943.0	943.0	942.9	**A** sym. NbO_2 str.
893.0	893.0	893.0	**A** antisym. NbO_2 str.
644.9	626.9	635.0	**A** CO_2 bend.
641.0	622.8	631.4	**A** CO_2 bend.
2355.2	2289.1	2302.8	**B** antisym. CO_2 str.
2338.2	2273.4	2320.2	**B** antisym. CO_2 str.
927.8	927.8	927.7	**B** sym. NbO_2 str.
883.7	883.3	883.4	**B** antisym. NbO_2 str.
644.3	627.4	632.6	**B** CO_2 bend.
632.9	616.7	621.0	**B** CO_2 bend.
2007.8	1963.1	1961.2	**C** CO str.
1985.1	1940.6	1939.6	**C′** CO str.
928.4	928.4	912.6	**C** sym. NbO_2 str.
875.7	875.7	847.3	**C′** antisym. NbO_2 str.
871.7	871.6	844.3	**C** antisym. NbO_2 str.
2365.6	2299.7		**D** antisym. CO_2 str.
1887.5	1841.9	1851.1	**D** CO str.
1132.6	1122.7	1086.7	**D** CO str.
952.8	952.8	952.8	**D** sym. NbO_2 str.
910.3	910.3	910.2	**D** antisym. NbO_2 str.
672.4	662.6	653.4	**D** CO_2 bend.
1511.4	1473.0	1484.1	**E** antisym. CO_2 str.
1333.3	1309.1	1295.9	**E** sym. CO_2 str.
979.9	979.9	979.8	**E** sym. NbO_2 str.
939.3	939.3	939.3	**E** antisym. NbO_2 str.
803.6	794.9	777.1	**E** CO_2 bend.
978.5	978.5	978.5	NbO
957.2	957.2	957.2	NbO_2 sym. str.
907.8	907.8	907.8	NbO_2 antisym. str.
2347.7	2282.1	2312.7	CO_2 antisym. str.
668.0	649.0	658.2	CO_2 bend.

inequivalent. The group **B** absorptions increased on annealing after $NbO_2(\eta^1\text{-OCO})$ and are favored with relatively high CO_2 concentrations. Two absorptions at 2355.2 and 2338.2 cm^{-1} were observed in the antisymmetric CO_2 stretching frequency region, indicating the involvement of two CO_2 subunits in species **B**. Therefore, the group **B** absorptions are assigned to the 1:2 $NbO_2(\eta^1\text{-OCO})_2$ complex.

Three absorptions were observed for species **C**. The 2007.8 cm^{-1} absorption shifted to 1963.1 cm^{-1} with $^{13}CO_2$ and to 1961.2 cm^{-1} with $C^{18}O_2$. The isotopic shifts indicate that the 2007.8 cm^{-1} absorption is due to a CO stretching vibration. The spectra from the experiments with the $^{12}CO_2$ + $^{13}CO_2$ and $C^{16}O_2$ + $C^{16}O^{18}O$ + $C^{18}O_2$ mixtures (Figure 5) clearly indicate that one CO fragment is involved in this mode. Therefore, the group **C** absorptions are assigned to the $NbO_2(\eta^1\text{-CO})$ complex, a carbonyl complex of NbO_2. The 928.4 and 871.7 cm^{-1} absorptions are symmetric and antisymmetric NbO_2 stretching vibrations. These two absorptions shifted to 912.6 and 844.3 cm^{-1} with $C^{18}O_2$, corresponding to the symmetric and antisymmetric $Nb^{16,18}O_2$ stretching vibrations. Besides these four absorptions, no additional absorptions were observed in the experiment with the $C^{16}O_2$ + $C^{16}O^{18}O$ + $C^{18}O_2$ mixture. These spectral features indicate that one O atom of the NbO_2 fragment in $NbO_2(\eta^1\text{-CO})$ is originated from CO_2, suggesting that species **C** is formed via the reaction of niobium monoxide with CO_2. Absorptions at 1985.1, and 875.7 cm^{-1} (labeled as **C′** in the figures) exhibit about the same isotopic spectral features as that of the NbO_2−CO absorptions. The upper absorption is due to a C−O stretching mode, and the low absorption is due to an antisymmetric NbO_2 stretching mode. The symmetric stretching mode is not observed due to weakness. These absorptions are favored in the experiments with high CO_2 concentrations and are tentatively assigned to the $NbO_2(\eta^1\text{-CO})(\eta^1\text{-OCO})$ complex.

Absorber **D** was produced under near-infrared light irradiation (λ > 800 nm) at the expense of the group **B** absorptions, which suggests that species **D** is due to a structural isomer of **B**. The observed isotopic shifts indicate that the 1887.5 and 1132.6 cm^{-1} absorptions are CO stretching vibrations. The doublet spectral features observed in the experiment with the $^{12}CO_2$ + $^{13}CO_2$ sample (Figure 5, trace c) and the quartet spectral features in the experiment using the $C^{16}O_2$ + $C^{16}O^{18}O$ + $C^{18}O_2$ mixture (Figure 5, trace e, quartet at 1887.5, 1881.6, 1857.4, and 1851.1 cm^{-1} for the upper mode and quartet at 1132.6, 1117.6, 1100.5, and 1081.0 cm^{-1} for the low mode) indicate that one CO_2 subunit with two inequivalent O atoms is involved in these two modes, which suggest the involvement of a CO_2 ligand with the η^2-C,O fashion. The observation of an additional antisymmetric CO_2 stretching vibration at 2365.6 cm^{-1} implies that species **D** involves another CO_2 subunit with the η^1-O coordination fashion. Accordingly, absorber **D** is assigned to the $NbO_2(\eta^1\text{-OCO})(\eta^2\text{-OC})O$ complex. The η^2-C,O mode on niobium center has previously been reported.[33]

Species **E** was produced under visible light irradiation (400 < λ < 580 nm) at the expense of the group **A** and **D** absorptions. The 1511.4 cm^{-1} absorption shifted to 1473.0 cm^{-1} with $^{13}CO_2$ and to 1484.1 cm^{-1} with $C^{18}O_2$. The isotopic frequency ratios ($^{12}C/^{13}C$, 1.0261; $^{16}O/^{18}O$, 1.0184) imply that this absorption is due to an antisymmetric CO_2 stretching vibration. The spectra from the experiments with the $^{12}CO_2$ + $^{13}CO_2$ and $C^{16}O_2$ + $C^{16}O^{18}O$ + $C^{18}O_2$ mixtures (Figure 6) clearly indicate that one CO_2 fragment with two equivalent O atoms is involved in this mode. The much weak 1333.3 cm^{-1} absorption is the corresponding symmetric stretching mode of the CO_2 fragment. These observations suggest the assignment of group **E** absorptions to $NbO_2(\eta^2\text{-O}_2\text{C})$ with CO_2 in an η^2-O,O fashion.

On the basis of above discussion, five niobium dioxide complexes including one carbonyl complex (**C**) and four carbon dioxide complexes (**A**, **B**, **D**, and **E**) were formed and characterized. The carbonyl complex has the lowest NbO_2 stretching frequencies. Among the four CO_2 complexes, the NbO_2 stretching frequencies increased following the trend $NbO_2(\eta^2\text{-O}_2\text{C})$ > $NbO_2(\eta^1\text{-OCO})(\eta^2\text{-OC})O$ > $NbO_2(\eta^1\text{-OCO})$ > $NbO_2(\eta^1\text{-OCO})_2$. In concert, the antisymmetric CO_2 stretching frequency increases almost in the reverse order. As will be discussed, the observed frequency shifts are a direct consequence of the nature of bonding interactions between NbO_2 and CO_2 in these complexes with different coordination modes.

To validate the experimental assignment, quantum chemical calculations using the density functional theory were performed. The optimized structures of the above-characterized species are shown in Figure 7. The $NbO_2(\eta^1\text{-OCO})$ complex (**A**) was

predicted to have a $^2A'$ ground state with C_s symmetry. The $NbO_2(\eta^1\text{-}OCO)_2$ complex (**B**) has a C_2 symmetry. Both complexes were predicted to have nearly linear bond angles of the CO_2 ligands. The η^2-O,O bonded $NbO_2(\eta^2\text{-}O_2C)$ complex (**E**) was predicted to have a C_{2v} symmetry possessing a bent CO_2 ligand with an OCO bond angle of 126.5°. The $NbO_2(\eta^1\text{-}OCO)(\eta^2\text{-}OC)O$ complex (**D**) has a C_s symmetry with both CO_2 ligands lie in the same plane that is perpendicular to the NbO_2 plane. The η^2-C,O coordinated CO_2 ligand was calculated to be bent with a bond angle of 147.8°. The calculated vibrational frequencies and isotopic frequency shifts of these complexes are compared with the experimental values in Tables 2−6, respectively, which provide strong support for the identification of these complexes.

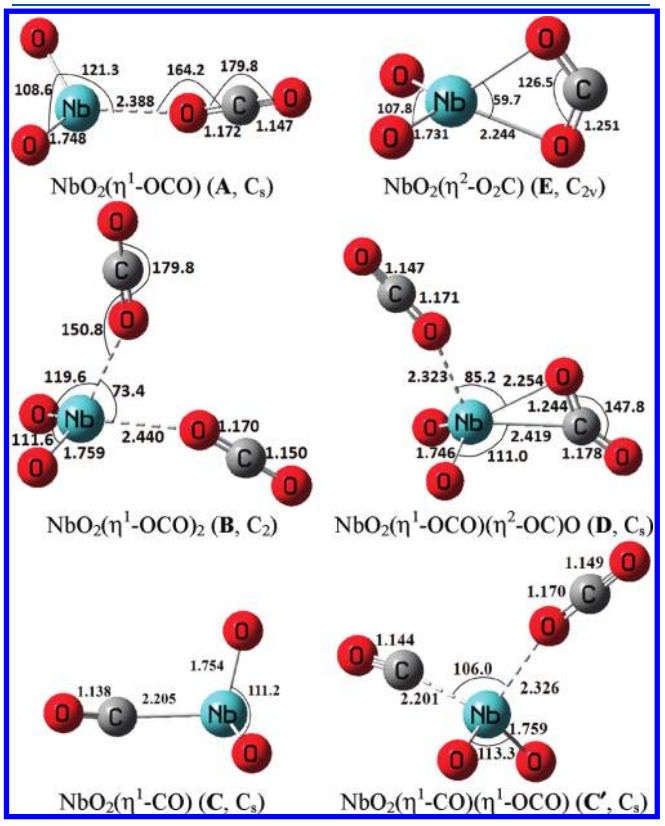

Figure 7. Optimized structures (bond lengths in angstroms, bond angles in degrees) of the species observed from the NbO_2 + CO_2 reactions.

All of the above characterized niobium dioxide-carbon dioxide complexes (**A**, **B**, **D**, **E**) can be viewed as being formed via the ground state of NbO_2 ($^2A_1$) and CO_2. Natural bond orbital (NBO) analysis (Table 7) indicated that the η^1-O coordinated CO_2 ligand serves as an electron donor, whereas both the η^2-C,O and η^2-O,O coordinated CO_2 ligands act as electron acceptors. Both the two η^1-O bound complexes are weak donor−acceptor complexes with the oxygen of CO_2 donates its lone-pair electrons to the empty 4d orbital of Nb. On the other hand, the $NbO_2(\eta^2\text{-}O_2C)$ complex can be described as $[NbO_2]^+[CO_2]^-$, a charge-transfer complex in which the charge on the CO_2 ligand is −0.52e. Both the observed vibrational frequencies and the predicted geometry of the CO_2 subunit of the $NbO_2(\eta^2\text{-}O_2C)$ complex are very close to those of free CO_2^- anion.[34] Molecular orbital analysis indicated that the unpaired electron is localized on the molecular orbital that is mainly π^* orbital of CO_2 in character. The η^2-C,O coordinated CO_2 ligand in $NbO_2(\eta^1\text{-}OCO)(\eta^2\text{-}OC)O$ is less activated than that in $NbO_2(\eta^2\text{-}O_2C)$. As can be seen in Figure 7, the two CO bonds of the η^2-C,O coordinated CO_2 ligand are quite inequivalent. The terminal one has a bond length of 1.178 Å, while the coordinated one has a much longer bond length of 1.244 Å, about the same as that in $NbO_2(\eta^2\text{-}O_2C)$. Molecular orbital and NBO analysis showed that there is bonding interaction between the singly occupied (SOMO) a_1 orbital of NbO_2 (primarily a hybrid of the Nb 5s and 4d orbitals) and one of the empty π^* orbital of CO_2. NBO analysis showed that the η^2-C,O coordinated CO_2 also draws electrons from NbO_2 but to a much less degree than the η^2-O,O coordinated CO_2 (Table 7).

Three different CO_2 coordination modes on the niobium metal center including η^1-O, η^2-C,O and η^2-O,O are identified von the above characterized four niobium dioxide−carbon dioxide complexes. Transition metal carbon dioxide complexes serve as simple models in understanding the structural and functional properties of catalytic surface bound intermediates. Since the report of the first structurally characterized CO_2 complex with a η^2-C,O coordination mode in $Ni(PCy_3)_2(\eta^2\text{-}CO_2)$ (Cy = cyclohexyl),[35] CO_2 has been observed to bind to a mononuclear transition metal center in three different modes.[2] Besides the η^2-C,O mode, the η^1-O and η^1-C modes have also been characterized in many transition metal carbon dioxide complexes.[36,37] The η^2-O,O mode on mononuclear transition

Table 2. Observed Neon Matrix and Calculated (B3LYP/6-311+G(d)/SDD) Vibrational Frequencies (cm^{-1}) for NbO_2-(η^1-OCO) (A)

	$NbO_2(\eta^1\text{-}OCO)$		$NbO_2(\eta^1\text{-}O^{13}CO)$		$NbO_2(\eta^{1}\text{-}^{18}OC^{18}O)$	
mode	obsd	calcd[a]	obsd	calcd	obsd	calcd
antisym. CO_2 str.	2371.5	2447.5 (1072)	2305.0	2377.8	2336.1	2410.2
sym. CO_2 str.	1376.1	1383.5 (18)	1366.8	1383.4	1318.9	1304.4
sym. NbO_2 str.	943.0	950.9 (115)	943.0	950.9	942.9	950.9
antisym. NbO_2 str.	893.0	908.0 (293)	893.0	908.0	893.0	908.0
CO_2 bend.	644.9	639.6 (34)	626.9	621.5	635.0	629.8
CO_2 bend.	641.0	634.6 (36)	622.8	616.5	631.4	624.8

[a] The intensities are listed in parentheses in km/mol. Only the vibrations above 400 cm^{-1} are listed. The other modes were calculated at 26.8, 28.3, 83.1, 98.6, 164.2, and 321.7 cm^{-1}. The symmetric and antisymmetric NbO_2 stretching modes of ground state NbO_2 were predicted at 972.8 and 927.4 cm^{-1}, the frequencies of CO_2 were calculated to be 2420.0, 1373.0, and 668.6 cm^{-1}.

dx.doi.org/10.1021/jp208291g |J. Phys. Chem. A 2011, 115, 14361–14369

Table 3. Observed Neon Matrix and Calculated (B3LYP/6-311+G(d)/SDD) Vibrational Frequencies (cm^{-1}) for NbO_2-(η^1-OCO)$_2$ (B)

	$NbO_2(\eta^1\text{-}OCO)_2$		$NbO_2(\eta^1\text{-}O^{13}CO)_2$		$NbO_2(\eta^1\text{-}^{18}OC^{18}O)_2$	
mode	obsd	calcd[a]	obsd	calcd	obsd	calcd
antisym. CO_2 str.	2355.2	2447.8 (414)	2289.1	2378.0	2302.8	2410.4
antisym. CO_2 str.	2338.2	2429.1 (1979)	2273.4	2359.8	2320.2	2392.2
sym. CO_2 str.		1374.7 (0)		1374.6		1296.0
sym. CO_2 str.		1372.7 (6)		1372.6		1294.1
sym. NbO_2 str.	927.8	934.9 (103)	927.8	934.9	927.7	934.9
antisym. NbO_2 str.	883.7	893.9 (336)	883.3	893.9	883.4	893.9
CO_2 bend.	644.3	643.4 (60)	627.4	625.2	632.6	633.5
CO_2 bend.		642.5 (1)		624.3		632.5
CO_2 bend.		614.5 (3)		596.9		605.4
CO_2 bend.	632.9	613.0 (79)	616.7	595.6	621.0	603.6

[a] The intensities are listed in parentheses in km/mol. Only the vibrations above 400 cm^{-1} are listed. The other modes were calculated at 28.2, 34.7, 35.5, 47.7, 76.4, 81.8, 107.3, 112.0, 147.9, 162.6, and 308.0 cm^{-1}.

Table 4. Observed Neon Matrix and Calculated (B3LYP/6-311+G(d)/SDD) Vibrational Frequencies (cm^{-1}) for NbO_2-(η^1-CO) (C)

	$NbO_2(\eta^1\text{-}CO)$		$NbO_2(\eta^1\text{-}^{13}CO)$		$Nb^{16}O^{18}O(\eta^1\text{-}C^{18}O)$	
mode	obsd	calcd[a]	obsd	calcd	obsd	calcd
CO str.	2007.8	2089.0 (1586)	1963.1	2041.9	1961.2	2039.4
sym. NbO_2 str.	928.4	941.9 (77)	928.4	941.9	912.6	926.9
antisym. NbO_2 str.	871.7	891.8 (260)	871.6	891.8	844.3	862.6

[a] The intensities are listed in parentheses in km/mol. Only the vibrations above 400 cm^{-1} are listed. The other modes were calculated at 100.3, 112.8, 274.9, 320.6, 324.5, and 357.7 cm^{-1}.

Table 5. Observed Neon Matrix and Calculated (B3LYP/6-311+G(d)/SDD) Vibrational Frequencies (cm^{-1}) for NbO_2-(η^1-OCO)(η^2-C,O)O (D)

	$NbO_2(\eta^1\text{-}OCO)(\eta^2\text{-}C,O)O$		$NbO_2(\eta^1\text{-}O^{13}CO)(\eta^2\text{-}^{13}C,O)O$		$NbO_2(\eta^1\text{-}C^{18}O_2)(\eta^2\text{-}C,^{18}O)^{18}O$	
mode	obsd	calcd[a]	obsd	calcd	obsd	calcd
antisym. CO_2 str.	2365.6	2459.5 (1167)	2299.7	2389.5		2422.0
CO str.	1887.5	2006.7 (558)	1841.9	1952.9	1851.1	1971.5
sym. CO_2 str.		1393.9 (28)		1393.9		1314.1
CO str.	1132.6	1175.7 (167)	1122.7	1169.6	1086.7	1117.8
sym. NbO_2 str.	952.8	960.1 (111)	952.8	960.1	952.8	959.9
antisym. NbO_2 str.	910.3	924.8 (269)	910.3	924.8	910.2	924.8
CO_2 bend	672.4	661.9 (319)	662.6	649.6	653.4	642.7
CO_2 bend		641.6 (32)		623.3		631.8
CO_2 bend		640.3 (23)		622.2		630.4
CO_2 bend		486.9 (8)		471.9		481.4

[a] The intensities are listed in parentheses in km/mol. Only the vibrations above 400 cm^{-1} are listed. The other modes were calculated at 7.5, 19.2, 79.4, 82.6, 116.7, 128.3, 145.5, 174.2, 235.6, 284.0, and 353.0 cm^{-1}.

metal center has never been experimentally reported. However, the negatively charged CO_2^- anion has been proposed to be bound on some transition metal surfaces with both oxygen atoms, which exhibits CO_2 vibrational band positions close to those of $NbO_2(\eta^2\text{-}O_2C)$ characterized here.[38]

Pulsed laser evaporation of bulk Nb_2O_5 target followed by condensation with CO_2 in excess neon at 4 K formed only the NbO and NbO_2 molecules. Annealing the deposited matrix sample allows the CO_2 molecules to diffuse and react with the NbO and NbO_2 molecules. The experimental observations clearly demonstrate the $NbO_2 + CO_2$ reaction mechanism outlined in Scheme 1.

It is quite interesting to note that the primarily formed η^1-O bound complexes show different isomerization reactions. The 1:1 complex rearranged to the η^2-O,O bound $NbO_2(\eta^2\text{-}O_2C)$ isomer under visible light irradiation, whereas the 1:2 complex isomerized to the $NbO_2(\eta^1\text{-}OCO)(\eta^2\text{-}OC)O$ complex under IR

dx.doi.org/10.1021/jp208291g |J. Phys. Chem. A 2011, 115, 14361–14369

Table 6. Observed Neon Matrix and Calculated (B3LYP/6-311+G(d)/SDD) Vibrational Frequencies (cm^{-1}) for NbO_2-(η^2-O_2C) (E)

	$NbO_2(\eta^2\text{-}O,O)C$		$NbO_2(\eta^2\text{-}O,O)^{13}C$		$NbO_2(\eta^2\text{-}^{18}O,^{18}O)C$	
mode	obsd	calcd[a]	obsd	calcd	obsd	calcd
antisym. CO_2 str.	1511.4	1566.7 (449)	1473.0	1525.5	1484.1	1538.0
sym. CO_2 str.	1333.3	1323.0 (3)	1309.1	1302.2	1295.9	1279.6
sym. NbO_2 str.	979.9	987.2 (129)	979.9	987.2	979.8	987.0
antisym. NbO_2 str.	939.3	955.5 (264)	939.3	955.4	939.3	955.4
CO_2 bend.	803.6	769.8 (10)	794.9	759.3	777.1	739.8

[a] The intensities are listed in parentheses in km/mol. Only the vibrations above 400 cm^{-1} are listed. The other modes were calculated at 98.7, 115.3, 150.1, 287.3, 332.7, 394.9, and 395.1 cm^{-1}.

Table 7. Natural Bond Orbital Charge Analysis (B3LYP/6-311+G(d)/SDD) for the Complexes Mentioned in the Text

complex	η^1-CO_2	η^2-CO_2	NbO_2
$NbO_2(\eta^1\text{-OCO})$ (**A**)	0.075e		−0.075e
$NbO_2(\eta^1\text{-OCO})_2$ (**B**)	0.074e		−0.149e
$NbO_2(\eta^1\text{-CO})$ (**C**)		0.032e[a]	−0.032e
$NbO_2(\eta^1\text{-CO})(\eta^1\text{-OCO})$ (**C′**)	0.111e	0.019e[a]	−0.130e
$NbO_2(\eta^1\text{-OCO})(\eta^2\text{-OC})O$ (**D**)	0.128e	−0.289e	0.161e
$NbO_2(\eta^2\text{-}O_2C)$ (**E**)		−0.519e	0.519e
$NbO_2(\eta^1\text{-OCO})$ (η^2-O_2C)	0.137e	−0.521e	0.384e
$NbO_2(\eta^2\text{-OC})O$		−0.202e	0.202e

[a] Charge of the CO ligand.

Scheme 1

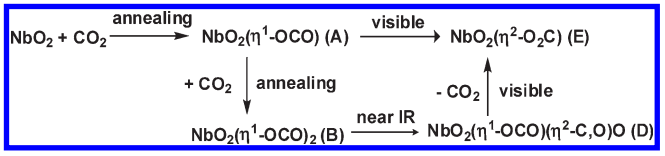

excitation. The potential energy profiles for the above-mentioned reactions calculated at the B3LYP level of theory are shown in Figures 8 and 9, respectively. In the 1:1 reaction system, the η^1-O complex is the most stable structure. Formation of the η^2-O,O bound isomer is endothermic and proceeds via the η^2-C,O bound intermediate with a barrier of 15.2 kcal/mol. The $NbO_2(\eta^2\text{-OC})O$ isomer cannot be observed since it is unstable as its rearrangement to $NbO_2(\eta^1\text{-OCO})$ is almost barrierless (Figure 8). In the 1:2 reaction system, the $NbO_2(\eta^1\text{-OCO})(\eta^2\text{-OC})O$ structure is the most stable structure. The η^1-O to η^2-C,O transfer process was predicted to have a very low barrier, which is in accord with experimental observation that near IR excitation is sufficient to initiate this isomerization reaction. Apparently, there is cooperative effect between the η^1-O and η^2 ligands in the 1:2 complexes. The η^1-O ligand donates electrons to Nb whereas the η^2 ligand draws electrons from NbO_2.

The isotopic substitution experimental results indicate that the ground state NbO molecule reacted with CO_2 to form the $NbO_2(\eta^1\text{-CO})$ complex spontaneously on annealing, reaction 1:

$$NbO(^4\Sigma) + CO_2 \rightarrow NbO_2(\eta^1\text{-CO})(^2A') \quad \Delta E = -34.7 \text{ kcal/mol} \qquad (1)$$

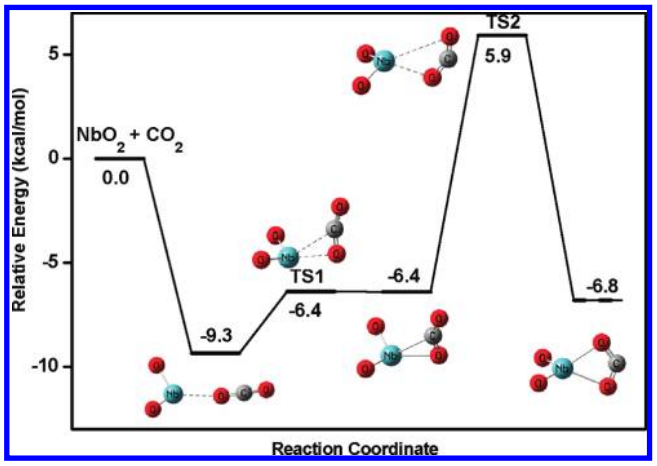

Figure 8. Potential-energy profile (ZPE corrected, in kcal mol^{-1}) for the NbO_2 + CO_2 reaction calculated at the B3LYP/6-311+G(d)/SDD level of theory.

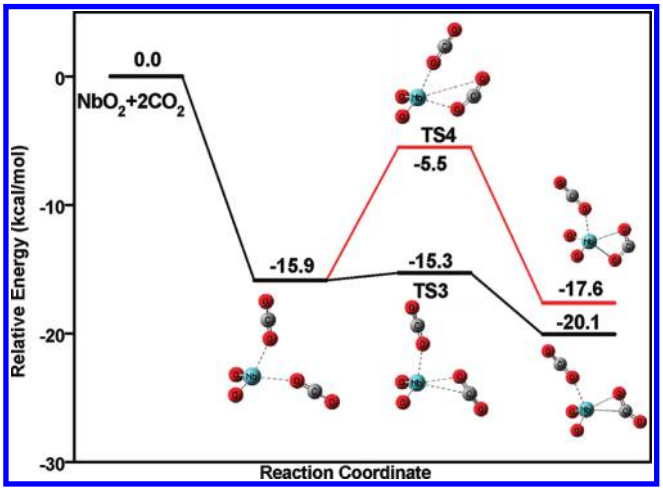

Figure 9. Potential-energy profile (ZPE corrected, in kcal mol^{-1}) for the NbO_2 + $2CO_2$ reaction calculated at the B3LYP/6-311+G(d)/SDD level of theory.

The potential energy profile along the NbO + CO_2 → NbO_2-(η^1-CO) reaction path was calculated, and the results are shown in Figure 10. The reaction was predicted to proceed via the $NbO(\eta^1\text{-OCO})$ and $NbO(\eta^2\text{-OC})O$ complex intermediates. Because NbO has a quartet ground state, while the $NbO_2(\eta^1\text{-CO})$

dx.doi.org/10.1021/jp208291g |J. Phys. Chem. A 2011, 115, 14361–14369

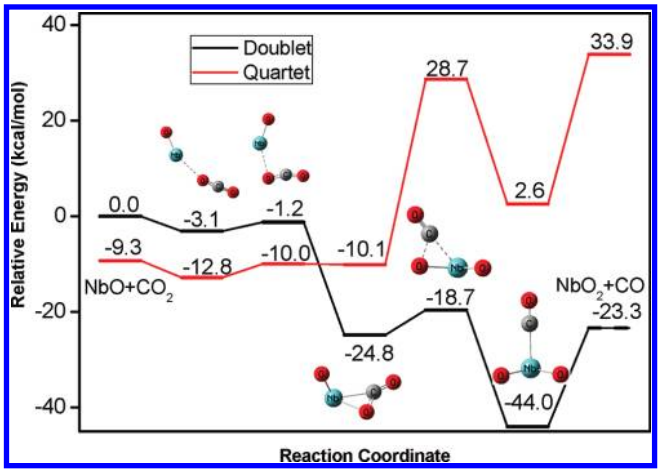

Figure 10. Potential-energy profile (ZPE corrected, in kcal/mol) for the NbO + CO_2 reaction calculated at the B3LYP/6-311+G(d)/SDD level of theory.

complex has a doublet ground state, there is spin crossing for reaction 1. The overall reaction was predicted to be exothermic by 34.7 kcal/mol and proceeds with negligible activation energy. Experimentally, the $NbO_2(\eta^1\text{-}CO)$ complex absorptions increased on annealing, and the $NbO(\eta^1\text{-}OCO)$ and $NbO(\eta^2\text{-}OC)O$ intermediates were not observed. CO_2 reduction to CO bound on metal center has been reported in many systems.[39] In general, CO_2 can be reduced to CO at electron-rich metal centers with the concomitant formation of strong metal−oxygen bond to compensate for overcoming the high enthalpy of the C═O bond of carbon dioxide.

CONCLUSIONS

Carbon dioxide coordination and activation by niobium monoxide and dioxide molecules were investigated by matrix isolation infrared spectroscopy as well as theoretical calculations. The ground state NbO molecule reacted with carbon dioxide in solid neon to form the $NbO_2(\eta^1\text{-}CO)$ complex spontaneously on annealing, in which CO_2 is reduced to CO bound on a NbO_2 center. Theoretical calculations indicate that this carbon dioxide activation process is both thermodynamically exothermic and kinetically facile. The niobium dioxide molecule reacted with carbon dioxide in solid neon in formation the η^1-O bound $NbO_2(\eta^1\text{-}OCO)$ and $NbO_2(\eta^1\text{-}OCO)_2$ complexes on annealing. The $NbO_2(\eta^1\text{-}OCO)$ complex rearranged to the η^2-O,O bound $NbO_2(\eta^2\text{-}O_2C)$ isomer under visible light irradiation, while the $NbO_2(\eta^1\text{-}OCO)_2$ complex isomerized to the $NbO_2(\eta^1\text{-}OCO)\text{-}(\eta^2\text{-}OC)O$ structure involving an η^2-C,O ligand under IR excitation. Natural bond orbital analysis indicated that the η^1-O coordinated CO_2 ligand serves as an electron donor, whereas both the η^2-C,O and η^2-O,O coordinated CO_2 ligands act as electron acceptors in these niobium dioxide−carbon dioxide complexes.

AUTHOR INFORMATION

Corresponding Authors

*Fax: (+86) 21-6564-3532. E-mail: mfzhou@fudan.edu.cn (M.Z.); lizhenhua@fudan.edu.cn (Z.H.L.).

ACKNOWLEDGMENT

This work was supported by NKBRSF (2010CB732306) and NSFC (20933030 and 21173053).

REFERENCES

(1) (a) Sakakura, T.; Choi, J. C.; Yasuda, H. *Chem. Rev.* **2007**, *107*, 2365. (b) Arakawa, H.; Aresta, M.; Armor, J. N.; Barteau, M. A.; Beckman, E. J.; Bell, A. T.; Bercaw, J. E.; Creutz, C.; Dinjus, E.; Dixon, D. A.; Domen, K.; DuBois, D. L.; Eckert, J.; Fujita, E.; Gibson, D. H.; Goddard, W. A.; Goodman, D. W.; Keller, J.; Kubas, G. J.; Kung, H. H.; Lyons, J. E.; Manzer, L. E.; Marks, T. J.; Morokuma, K.; Nicholas, K. M.; Periana, R.; Que, L.; Rostrup-Nielson, J.; Sachtler, W. M. H.; Schmidt, L. D.; Sen, A.; Somorjai, G. A.; Stair, P. C.; Stults, B. R.; Tumas, W. *Chem. Rev.* **2001**, *101*, 953. (c) Aresta, M.; Dibenedetto, A. *Dalton Trans.* **2007**, 2975.

(2) (a) Gibson, D. H. *Chem. Rev.* **1996**, *96*, 2063. (b) Leitner, W. *Coord. Chem. Rev.* **1996**, *153*, 257.

(3) (a) He, L. N.; Wang, J. Q.; Wang, L. J. *Pure Appl. Chem.* **2009**, *81*, 2069. (b) Yin, X. L.; Moss, J. R. *Coord. Chem. Rev.* **1999**, *181*, 27. (c) Federsel, C.; Jackstell, R.; Beller, M. *Angew. Chem., Int. Ed.* **2010**, *49*, 6254. (d) Coates, G. W.; Moore, D. R. *Angew. Chem., Int. Ed.* **2004**, *43*, 6618.

(4) Dheandhanoo, S.; Chatterjee, B. K.; Johnson, R. *J. Chem. Phys.* **1985**, *83*, 3327.

(5) Irikura, K. K.; Beauchamp, J. L. *J. Phys. Chem.* **1991**, *95*, 8344.

(6) Wesendrup, R.; Schwarz, H. *Angew. Chem., Int. Ed.* **1995**, *34*, 2033.

(7) Sievers, M. R.; Armentrout, P. B. *J. Chem. Phys.* **1995**, *102*, 754.

(8) (a) Sievers, M. R.; Armentrout, P. B. *Int. J. Mass Spectrom.* **1998**, *179/180*, 103. (b) Griffin, J. B.; Armentrout, P. B. *J. Chem. Phys.* **1998**, *108*, 8075. (c) Sievers, M. R.; Armentrout, P. B. *J. Phys. Chem. A* **1998**, *102*, 10754. (d) Sievers, M. R.; Armentrout, P. B. *Inorg. Chem.* **1999**, *38*, 397. (e) Zhang, X. G.; Armentrout, P. B. *J. Phys. Chem. A* **2003**, *107*, 8904.

(9) Koyanagi, G. K.; Bohme, D. K. *J. Phys. Chem. A* **2006**, *110*, 1232.

(10) (a) Campbell, M. L. *Phys. Chem. Chem. Phys.* **1999**, *1*, 3731. (b) Campbell, M. L. *Chem. Phys. Lett.* **2000**, *330*, 547.

(11) Larsson, R.; Mascetti, J. *React. Kinet. Catal. Lett.* **2005**, *85*, 107.

(12) (a) Mascetti, J.; Tranquille, M. *J. Phys. Chem.* **1988**, *92*, 2177. (b) Galan, F.; Fouassier, M.; Tranquille, M.; Mascetti, J.; Papai, I. *J. Phys. Chem. A* **1997**, *101*, 2626. (c) Mascetti, J.; Galan, F.; Papai, I. *Coord. Chem. Rev.* **1999**, *190−192*, 557.

(13) (a) Souter, P. F.; Andrews, L. *Chem. Commun.* **1997**, 777. (b) Souter, P. F.; Andrews, L. *J. Am. Chem. Soc.* **1997**, *119*, 7350.

(14) (a) Zhou, M. F.; Andrews, L. *J. Am. Chem. Soc.* **1998**, *120*, 13230. (b) Zhou, M. F.; Andrews, L. *J. Phys. Chem. A* **1999**, *103*, 2066. (c) Zhou, M. F.; Liang, B. Y.; Andrews, L. *J. Phys. Chem. A* **1999**, *103*, 2013.

(15) (a) Zhang, L. N.; Wang, X. F.; Chen, M. H.; Qin, Q. Z. *Chem. Phys.* **2000**, *254*, 231. (b) Chen, M. H.; Wang, X. F.; Zhang, L. N.; Qin, Q. Z. *J. Phys. Chem. A* **2000**, *104*, 7010. (c) Wang, X. F.; Chen, M. H.; Zhang, L. N.; Qin, Q. Z. *J. Phys. Chem. A* **2000**, *104*, 758.

(16) (a) Liang, B. Y.; Andrews, L. *J. Phys. Chem. A* **2002**, *106*, 595. (b) Liang, B. Y.; Andrews, L. *J. Phys. Chem. A* **2002**, *106*, 4042.

(17) Andrews, L.; Zhou, M. F.; Liang, B. Y.; Li, J.; Bursten, B. E. *J. Am. Chem. Soc.* **2000**, *122*, 11440.

(18) Jiang, L.; Zhang, X. B.; Han, S.; Xu, Q. *Inorg. Chem.* **2008**, *47*, 4826.

(19) (a) Sodupe, M.; Branchadell, V.; Oliva, A. *J. Phys. Chem.* **1995**, *99*, 8567. (B) Sodupe, M.; Branchadell, V.; Rosi, M.; Bauschlicher, C. W., Jr. *J. Phys. Chem. A* **1997**, *101*, 7854.

(20) (a) Hwang, D. Y.; Mebel, A. M. *Chem. Phys. Lett.* **2002**, *357*, 51. (b) Hwang, D. Y.; Mebel, A. M. *J. Chem. Phys.* **2002**, *116*, 5633. (c) Hwang, D. Y.; Mebel, A. M. *J. Phys. Chem. A* **2000**, *104*, 11622.

(21) (a) Papai, I.; Schubert, G.; Hannachi, Y.; Mascetti, J. *J. Phys. Chem. A* **2002**, *106*, 9551. (b) Papai, I.; Mascetti, J.; Fournier, R. *J. Phys. Chem. A* **1997**, *101*, 4465. (c) Papai, I.; Hannachi, Y.; Gwizdala, S.; Mascetti, J. *J. Phys. Chem. A* **2002**, *106*, 4181. (d) Hannachi, Y.; Mascetti, J.; Stirling, A.; Papai, I. *J. Phys. Chem. A* **2003**, *107*, 6708.

(22) (a) Wang, Y. C.; Yang, X. Y.; Geng, Z. Y.; Liu, Z. Y.; Chen, X. X.; Gao, L. G. *Acta. Chim. Sin.* **2006**, *64*, 2310. (b) Dai, G. L.; Wang, C. F. *THEOCHEM* **2009**, *909*, 122.

(23) (a) Chen, X. Y.; Zhao, Y. X.; Wang, S. G. *J. Phys. Chem. A* **2006**, *110*, 3552. (b) Musaev, D. G.; Irle, S.; Lin, M. C. *J. Phys. Chem. A* **2007**, *111*, 6665.
(24) Hossain, E.; Rothgeb, D. W.; Jarrold, C. C. *J. Chem. Phys.* **2010**, *133*, 024305.
(25) (a) Zhou, M. F.; Zhang, L. N.; Shao, L. M.; Wang, W. N.; Fan, K. N.; Qin, Q. Z. *J. Phys. Chem. A* **2001**, *105*, 10747. (b) Zhou, M. F.; Zhang, L. N.; Qin, Q. Z. *J. Phys. Chem. A* **2001**, *105*, 6407.
(26) (a) Wang, G. J.; Chen, M. H.; Zhou, M. F. *J. Phys. Chem. A* **2004**, *108*, 11273. (b) Wang, G. J.; Gong, Y.; Chen, M. H.; Zhou, M. F. *J. Am. Chem. Soc.* **2006**, *128*, 5974. (c) Wang, G. J.; Chen, M. H.; Zhao, Y. Y.; Zhou, M. F. *Chem. Phys.* **2006**, *322*, 354. (d) Wang, G. J.; Lai, S. X.; Chen, M. H.; Zhou, M. F. *J. Phys. Chem. A* **2005**, *109*, 9514. (e) Huang, Y. F.; Zhao, Y. Y.; Zheng, X. M.; Zhou, M. F. *J. Phys. Chem. A* **2010**, *114*, 2476.
(27) (a) Zhou, M. F.; Wang, C. X.; Li, Z. H.; Zhuang, J.; Zhao, Y. Y.; Zheng, X. M.; Fan, K. N. *Angew. Chem., Int. Ed.* **2010**, *49*, 7757. (b) Wang, C. X.; Zhuang, J.; Wang, G. J.; Chen, M. H.; Zhao, Y. Y.; Zheng, X. M.; Zhou, M. F. *J. Phys. Chem. A* **2010**, *114*, 8083. (c) Zhao, Y. Y.; Huang, Y. F.; Zheng, X. M.; Zhou, M. F. *J. Phys. Chem. A* **2010**, *114*, 5779. (D) Zhou, M. F.; Wang, C. X.; Zhuang, J.; Zhao., Y. Y.; Zheng, X. M. *J. Phys. Chem. A* **2011**, *115*, 39.
(28) (a) Wang, G. J.; Zhou, M. F. *Int. Rev. Phys. Chem.* **2008**, *27*, 1. (b) Zhou, M. F.; Andrews, L.; Bauschlicher, C. W., Jr. *Chem. Rev.* **2001**, *101*, 1931.
(29) (a) Becke, A. D. *J. Chem. Phys.* **1993**, *98*, 5648. (b) Lee, C.; Yang, W.; Parr, R. G. *Phys. Rev. B* **1988**, *37*, 785.
(30) (a) Dolg, M.; Stoll, H.; Preuss, H. *J. Chem. Phys.* **1989**, *90*, 1730. (b) Andrae, D.; Haussermann, U.; Dolg, M.; Stoll, H.; Preuss, H. *Theor. Chim. Acta.* **1990**, *77*, 123.
(31) Frisch, M. J.; Trucks, G. W.; Schlegel, H. B.; Scuseria, G. E.; Robb, M. A.; Cheeseman, J. R.; Scalmani, G.; Barone, V.; Mennucci, B.; Petersson, G. A.; Nakatsuji, H.; Caricato, M.; Li, X.; Hratchian, H. P.; Izmaylov, A. F.; Bloino, J.; Zheng, G.; Sonnenberg, J. L.; Hada, M.; Ehara, M.; Toyota, K.; Fukuda, R.; Hasegawa, J.; Ishida, M.; Nakajima, T.; Honda, Y.; Kitao, O.; Nakai, H.; Vreven, T.; Montgomery, J. A., Jr.; Peralta, J. E.; Ogliaro, F.; Bearpark, M.; Heyd, J. J.; Brothers, E.; Kudin, K. N.; Staroverov, V. N.; Kobayashi, R.; Normand, J.; Raghavachari, K.; Rendell, A.; Burant, J. C.; Iyengar, S. S.; Tomasi, J.; Cossi, M.; Rega, N.; Millam, J. M.; Klene, M.; Knox, J. E.; Cross, J. B.; Bakken, V.; Adamo, C.; Jaramillo, J.; Gomperts, R.; Stratmann, R. E.; Yazyev, O.; Austin, A. J.; Cammi, R.; Pomelli, C.; Ochterski, J. W.; Martin, R. L.; Morokuma, K.; Zakrzewski, V. G.; Voth, G. A.; Salvador, P.; Dannenberg, J. J.; Dapprich, S.; Daniels, A. D.; Farkas, O.; Foresman, J. B.; Ortiz, J. V.; Cioslowski, J.; Fox, D. J. *Gaussian 09*, Revision A.02; Gaussian, Inc.: Wallingford, CT, 2009.
(32) (a) Zhou, M. F.; Andrews, L. *J. Phys. Chem. A* **1998**, *102*, 8251. (b) Gong, Y.; Zhou, M. F.; Andrews, L. *Chem. Rev.* **2009**, *109*, 6765.
(33) (a) Bristow, G. S.; Hitchcock, P. B.; Lappert, M. F. *J. Chem. Soc., Chem. Commun.* **1981**, 1145. (b) Fu, P. F.; Khan, M. A.; Nicholas, K. M. *J. Am. Chem. Soc.* **1992**, *114*, 6579. (c) Fu, P. F.; Khan, M. A.; Nicholas, K. M. *J. Organomet. Chem.* **1996**, *506*, 49.
(34) (a) Zhou, M. F.; Andrews, L. *J. Chem. Phys.* **1999**, *110*, 6820. (b) Thompson, W. E.; Jacox, M. E. *J. Chem. Phys.* **1999**, *111*, 4487.
(35) Aresta, M.; Nobile, C. F.; Albano, V. G.; Forni, E.; Manassero, M. *J. Chem. Soc., Chem. Commun.* **1975**, 636.
(36) (a) Gambarotta, S.; Arena, F.; Floriani, C.; Zanazzi, P. F. *J. Am. Chem. Soc.* **1982**, *104*, 5082. (b) Calabrese, J. C.; Herskovitz, T.; Kinney, J. B. *J. Am. Chem. Soc.* **1983**, *105*, 5914.
(37) Castro-Rodriguez, I.; Nakai, H.; Zakharov, L. N.; Rheingold, A. L.; Meyer, K. *Science* **2004**, *305*, 1757.
(38) (a) Bartos, B.; Freund, H. J.; Kuhlenbeck, H.; Neumann, M.; Lindner, H.; Miller, K. *Surf. Sci.* **1987**, *179*, 59. (b) Asscher, M.; Kao, C. T.; Somorjai, G. *J. Phys. Chem.* **1988**, *92*, 2711. (c) Brousseau, R.; Ellis, T. H.; Wang, H. *Chem. Phys. Lett.* **1991**, *177*, 118. (d) Xu, C.; Goodman, D. W. *J. Am. Chem. Soc.* **1995**, *117*, 12354. (e) He, H. Y.; Zapol, P.; Curtiss, L. A. *J. Phys. Chem. C* **2010**, *114*, 21474.
(39) (a) Castro-Rodriguez, I.; Meyer, K. *J. Am. Chem. Soc.* **2005**, *127*, 11242. (b) Lu, C. C.; Saouma, C. T.; Day, M. W.; Peters, J. C. *J. Am. Chem. Soc.* **2007**, *129*, 4. (c) Laitar, D. S.; Muller, P.; Sadighi, J. P. *J. Am. Chem. Soc.* **2005**, *127*, 17196.